PCCP

Accepted Manuscript

ROYAL SOCIETY OF CHEMISTRY

www.rsc.org/pccp

PCCP

ARTICLE

Designing voltage multipliers with nanofluidic diodes immersed in aqueous salt solutions

Received 00th January 20xx,
Accepted 00th January 20xx

DOI: 10.1039/x0xx00000x

www.rsc.org/

P. Ramirez,*[a] V. Gomez,[a] C. Verdia-Baguena,[b] S. Nasir,[c,d] M. Ali,[c,d] W. Ensinger[c] and S. Mafe[b]

Membranes with nanofluidic diodes allow the selective control of molecules in physiological salt solutions at ambient temperature. The electrical coupling of the membranes with conventional electronic elements such as capacitors suggests opportunities for the external monitoring of sensors and actuators. We demonstrate experimentally and theoretically the voltage multiplier functionality of simple electrical networks composed by membranes with conical nanopores coupled to load capacitors. The robust operation of half and full wave voltage multipliers is achieved under a broad range of experimental conditions (single pore and multipore membranes, electrolyte concentrations, voltage amplitudes, and solid-state capacitances). The designed voltage multipliers operate in liquid state and can be used in sensing devices because different electrical, optical, and chemical inputs are known to modulate the individual nanofluidic diode resistances in the electrical network.

1. Introduction

There is an increasing interest on signal processing with electrically coupled biological and solid-state electronics elements.[1-4] As in the case of biological cell membranes, the use of ions as signal carriers allows hybrid electrical circuits for sensing and monitoring biological systems in aqueous environments. While electrons and holes support the transfer of information in fixed architectures, ionic processors are dynamic structures such as membrane pores whose properties can be externally modulated by optical and electrical pulses in addition to thermal and chemical (pH and salt concentration) signals.[1,5-8]

Many electrochemical devices are based on electrolyte solutions immersed in micro and nanostructures with fixed charges. The external tuning of the interaction between the mobile electrolyte ions and the charges immobilized on pores allows a broad range of electrical responses. The analogies between electrolyte solutions and semiconductors, emphasized a long time ago by Reiss and Fuller,[9] suggest that external control of the electrical rectification in nanofluidic diodes may allow the translation of ionic responses into current and potential signals compatible with solid-state components. This fact should permit efficient signal processing using liquid-state, soft nanostructures, especially in those cases where the requirements on size, robustness, and speed are not critical. It should also be mentioned the rich surface chemistry which can be achieved using porous nanostructures.[5-7] Indeed, the different surface functionalizations allow highly selective control of specific molecules in a solution at ambient temperature and the biocompatibility of aqueous ionic circuits with physiological salt solutions offers opportunities for biologically-oriented sensors and actuators.[1,5,10-12]

In the case of nanofluidic diodes, however, a crucial step is to demonstrate the full functionality that can be achieved with simple electrical networks including macroscopic, conventional electronic elements (e.g., capacitors).[2,3,11] We have shown recently significant rectification of white noise signals using a single nanofluidic diode[13] and a nanoporous membrane.[14] We propose now to analyze experimentally and theoretically hybrid networks with simple connectivity. In particular, we demonstrate the robust operation of different half and full wave voltage multipliers under a range of electrolyte concentrations, voltage amplitudes, and solid-state capacitances. To this end, we have electrically coupled conventional load capacitors with single pore and multipore membranes having conical nanopores acting as potential dependent resistances. We emphasize that these voltage multipliers can also be used in sensing devices because electrical, optical, and chemical inputs are known to modulate the nanofluidic resistances.[5,10,12]

2. Experimental methods

2.1. Nanopore fabrication

Polyethylene terephthalate (PET) polymer foils (Hostaphan RN 12, Hoechst) of thickness 12 μm were irradiated with swift

[a] Departament de Física Aplicada, Universitat Politècnica de València, E-46022 València, Spain. E-mail: patraho@fis.upv.es
[b] Dept. de Física de la Tierra i Termodinàmica, Universitat de València, E-46100 Burjassot, Spain
[c] Dept. of Material- and Geo-Sciences, Materials Analysis, Technische Universität Darmstadt, D-64287 Darmstadt, Germany
[d] Materials Research Department, GSI Helmholtzzentrum für Schwerionenforschung, Planckstrasse 1, D-64291, Darmstadt, Germany

heavy (Au) ions (energy 11.4 MeV per nucleon) at UNILAC linear accelerator (GSI, Darmstadt). The tracks in the single pore and multipore membranes were converted to conical pores by means of asymmetric track-etching techniques.[15,16] These pores had 10 – 20 nm tip radii and 100 – 200 nm base radii, estimated from steady-state current (I) – potential (V) curves.[16] The multipore membrane pore density of the samples was 10^4 conical nanopores/cm^2 approximately. Carboxylate residues fixed to the wall surface of the pores were obtained at the end of the etching process. The groups were in ionized form at pH = 7, leading to an asymmetric charge distribution along the pore. Before and after each measurement, the pH value was checked by means of a Crison GLP22 pH-meter.

2.2. Electrical Measurements

In order to apply input voltages, as well as to measure output potential differences, Ag|AgCl electrodes immersed in the bathing solutions were used. Input voltage signals and electric currents were measured with a picoammeter/voltage source (Keithley 6487/E) and the voltage across the capacitors was measured with a multimeter (Keithley 2000/E).

3. Results and discussion

Fig. 1a schematically shows the experimental realization of the nanopore-based half wave voltage doubler. The device is based on polymer membranes with conical nanopores acting as fluidic diodes coupled with conventional electrolytic capacitors. The equivalent electrical circuit is depicted in Fig. 1b. Fig. 1c shows a typical steady state I-V curve for an individual multipore membrane used in the experiments. The membrane separated two identical KCl solutions of concentration c_0 = 0.1 M at pH = 7.

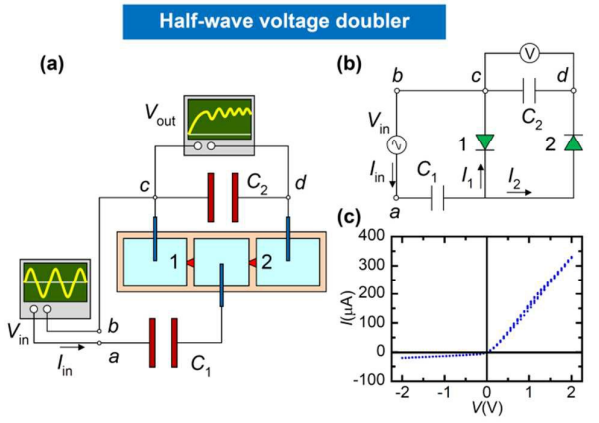

Fig.1 Scheme of the experimental set-up showing the half wave voltage doubler based on nanoporous membranes coupled with the electronic capacitors (a), the resulting equivalent electrical (b), and typical current-voltage curve obtained for an individual multipore membrane (c).

The voltages were applied on the electrode in the solution close to the narrow tip of the pores with the other electrode connected to ground. The pore charge asymmetry is responsible for the electrical rectification observed (control experiments at pH = 3 give no electrical rectification because the membrane fixed charge groups are in neutral form).[14] Indeed, the electrical resistance is low for $V > 0$ when the current enters the cone tip (high charge density and then high concentration of mobile ions) while this resistance is high for $V < 0$ when the current enters the cone base (low charge density).[16] Polymer films containing one single nanopore show similar rectifying I-V curves, with electric currents in the range of nA.[16]

Fig. 2 shows the experimental and theoretical results obtained for the half wave voltage multiplier in Fig. 1a.

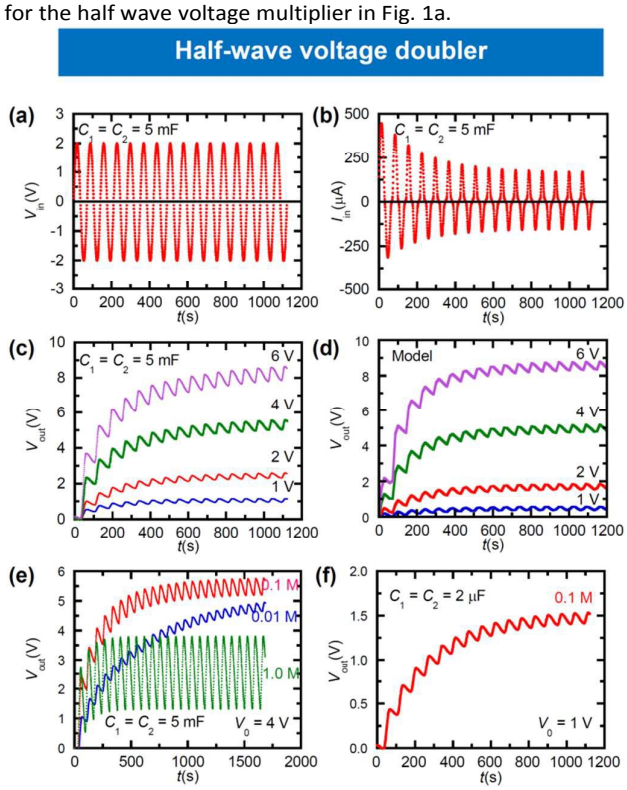

Fig.2 Experimental and theoretical results for the half wave voltage doubler in Fig. 1. Input sine wave (a), input AC current (b), rectified output voltage parametric in the input amplitude (c) and theoretical results (d), effect of the electrolyte concentration (e), effect of scaling using single-pore membranes (f).

The input signal $V_{in}(t)$ (Fig. 2a) is a sine wave of period T = 70 s and amplitude V_0. After a transient time, the resulting electric current $I_{in}(t)$ (Fig. 2b) entering the voltage doubler attains a steady AC regime. Fig. 2c shows the output voltage $V_{out}(t)$ parametrically in V_0. The output signals are DC voltages which attain a steady value, with a ripple of the same frequency as the input signal. The amplitude of the ripple increases with increasing the amplitude of the input signal, as in solid state circuits.[17] The steady value of the output voltage is lower than twice the amplitude of the input voltage because the fluidic diodes are not ideal.

The equations for the equivalent circuit of Fig. 1b are

$$V_{in} = \frac{q_1}{C_1} - V_1(-I_1), \quad (1)$$

$$V_{in} = \frac{q_1}{C_1} + V_2(I_2) + \frac{q_2}{C_2}, \quad (2)$$

$$I_{in} = \frac{dq_1}{dt}, \quad (3)$$

$$I_2 = \frac{dq_2}{dt}, \quad (4)$$

$$I_{in} = I_1 + I_2, \quad (5)$$

where q_1 and q_2 are the instantaneous charges on the plates of the capacitors of capacitances C_1 and C_2, respectively, and the voltage drops across the multipore membranes $V_1(-I_1)$ and $V_2(I_2)$ are obtained from the experimental *I-V* curves of the membrane samples used. Fig. 2d shows the theoretical results obtained after solving eqs. (1)-(5) with the initial boundary conditions $q_1(0) = q_2(0) = 0$ using Mathematica®. The model results correctly describe the experiments, including the increase of the ripple with the input signal amplitude, which supports further the circuit functionality of the nanofluidic diodes.

The experiments in Fig. 2e illustrate the effect of the electrolyte concentration on the output voltage. When the electrolyte concentration increases, the membrane electric resistance decreases. This fact leads to low transient times and high ripple amplitudes. The steady value attained by the output voltage reaches a maximum at intermediate electrolyte concentrations because the maximum rectification is achieved at concentrations close to 0.1 M.[16] Fig. 2f corresponds to single pore membranes, showing the effect of pore scaling on the electrical coupling. It is remarkable that similar results can be obtained with both single and multipore membranes by changing the capacitance values (to keep constant the product of effective resistance and the capacitance).

Fig. 3 shows the experimental set-up of the nanopore-based full wave voltage doubler multiplier coupled with the electronics capacitors (a) and the equivalent electrical circuit (b). The circuit components are the same as in Fig. 1.

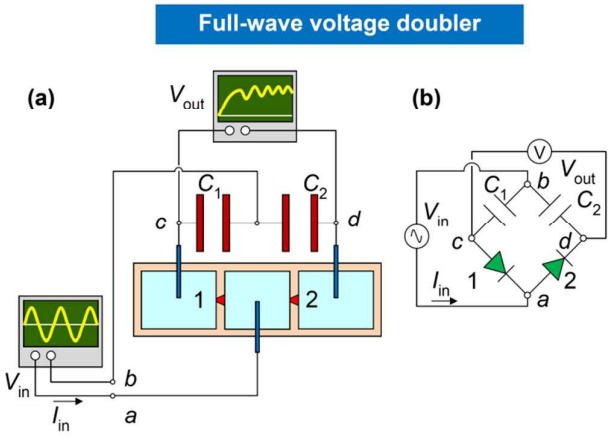

Fig.3 Scheme of the experimental set-up showing the full wave voltage doubler based on nanoporous membranes coupled with the electronics capacitors (a) and the equivalent electrical circuit (b).

In this case, the output voltage corresponds to the potential drop across the two capacitors. The experimental data obtained for the full wave voltage multiplier in Fig. 3 are shown in Fig. 4. Fig. 4a compares the results of the full wave and half wave voltage doublers. Note that the two circuits give the same steady value of the output voltage, as predicted by standard circuit theory.[17] The full wave ripple frequency is twice that of the half wave circuit. The full wave circuit allows decreasing both the transient time needed to attain the steady voltages and the ripple amplitude, which is also in agreement with the case of solid state diodes.[17] Figs. 4b-d illustrate the effect of the capacitance on the output voltage. Increasing the capacitance leads to higher output voltages and transient times while it gives lower ripple amplitudes. These experimental facts demonstrate again the circuit functionality of the nanofluidic diodes.

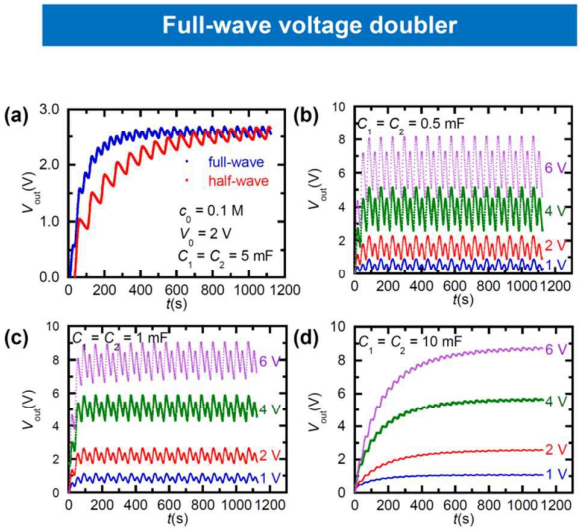

Fig.4 Experimental results for the output voltage using the full wave voltage doubler in Fig. 3 and c_0 = 0.1 M. Comparison with the case of the half wave voltage doubler (a) and effect of capacitance (b)-(d) parametrically in the amplitude V_0.

Fig. 5 corresponds to the experimental set-up of a new nanopore-based multiplier coupled with the electronic capacitors (a). In this case, two circuits similar to that in Fig. 1 are cascaded, giving the equivalent electrical circuit of a half wave voltage quadrupler (b). Fig. 5c compares the results of the half wave voltage doubler with the present voltage quadrupler. Note the significant increase of the steady value output voltage, obtained here at the price of increasing the transient time and the ripple amplitude. Taking together, the results of Figs. 2, 4, and 5 suggest that a robust electrical functionality can be achieved with hybrid circuits based on the coupling of the nanofluidic diodes with conventional solid state capacitors.

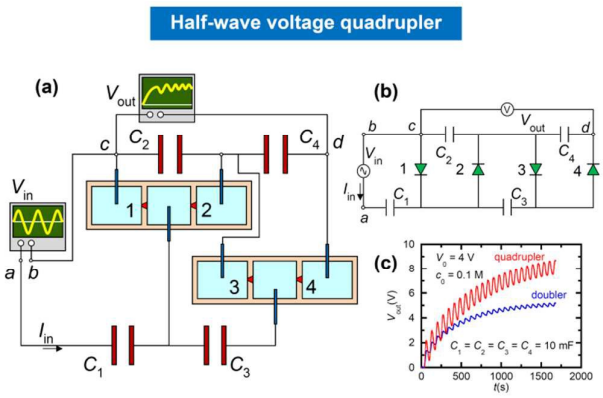

Fig.5 Scheme of the experimental set-up showing the voltage quadrupler based on nanoporous membranes coupled with the electronics capacitors (a), the equivalent electrical circuit (b), and comparison with the case of the half wave voltage doubler (c).

The liquid-state voltage multipliers demonstrated are based on the electrical rectification of alternating signals provided by the membranes. This rectification is supported by the individual nanopores and depends critically on the operating conditions. By using different functionalizations of the pore surface, this rectification can be externally modulated by the presence of specific analytes in the solution as well as by changing the analyte concentration (see e.g. Refs. 5, 10, and 12). Thus, the existing relation between sensing, pore rectification, and capacitor output potentials suggests that suitable functionalization of the nanofluidic diodes may allow the translation of ionic responses into current and potential signals compatible with the solid-state components in the networks.

The effect of sensing on the output voltage V_{out} can be simulated by decreasing the rectification of one of the membranes in the network, transforming it into a quasi-resistor whose resistance is that of the low current direction (the case of negative voltage in Fig. 1c). Incorporating this result in the circuit simulations immediately leads to significant decreases in V_{out}. Fig. 6 shows the results of the simulations in the case of the half wave multiplier of Fig. 1a, when the membrane sample 1 is transformed into a quasi-resistor due to the presence of a given analyte, resulting in an unbalanced network. In this way, sensing arises as a robust network output regardless of the individual event acting on a particular membrane or nanopore.

Conclusions

The design and characterization of simple electrical networks with micro and nanofluidic diodes performing collective tasks is of current technological interest. In particular, sensing and actuating with bioelectronics interfaces require the efficient connection of micro and nanofluidic elements to conventional electronic elements.[2-4,18] We have demonstrated experimentally and theoretically different voltage multipliers using electrical networks where nanoporous membranes with conical pores are effectively coupled to load capacitors. We have considered not only single nanopores but also multipore membranes in order to show the scaling effects on the electrical coupling. In all cases, the results are robust enough to indicate that a future integration of small scale networks into portable chip units should be feasible.[2,4,19] Note also that ions are much heavier than electrons, which suggests less vulnerability to undesired coupling effects between circuit components in close proximity.[1]

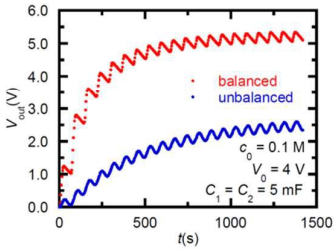

Fig. 6. The effect of decreasing, from the balanced to the unbalanced case, the rectification of one of the nanoporous membranes with respect to the others in the network is shown. The results correspond to the half-wave voltage multiplier.

The membranes incorporate nanofluidic diodes acting as potential dependent resistances which show a reproducible operation in half and full wave voltage multipliers circuits. This electrochemical functionality is demonstrated for different experimental conditions concerning electrolyte concentrations, voltage amplitudes, and capacitances. The coupling of the membranes with electronic elements should offer opportunities for external monitoring of biologically-oriented sensors and actuators at ambient temperature. Indeed, because different electrical, optical, and chemical inputs are known to modulate the nanofluidic diode resistance,[5] the designed voltage multipliers could be used in energy transduction[14] and nanopore-based sensing.[10,12]

Acknowledgements

We acknowledge the support from the Ministry of Economic Affairs and Competitiveness and FEDER (project MAT2015-65011-P) and the Generalitat Valenciana (project Prometeo/GV/0069 for Groups of Excellence).

Notes and references

1 H. Chun and T. D. Chung, *Annu. Rev. Anal. Chem.*, 2015, **8**, 441-462.
2 M. Tagliazucchi and I. Szleifer, *Mater. Today*, 2015, **18**, 131-142.
3 N. Misra and J. A. Martinez, S.-C. J. Huang, Y. Wang, P. Stroeve, C. P. Grigoropoulos and A. Noy, *Proc. Natl. Acad. Sci. U.S.A.*, 2009, **106**, 13780-13784.

4 S. Senapati, S. Basuray, Z. Slouka, L.-J. Cheng and H.-C. Chang, *Top. Curr. Chem.*, 2011, **304**, 153-169.
5 P. Ramirez, J. Cervera, M. Ali, W. Ensinger and S. Mafe, *ChemElectroChem*, 2014, **1**, 698-705.
6 C. R. Martin and Z. S. Siwy, *Science*, 2007, **317**, 331-332.
7 X. Hou and L. Jiang, *ACS Nano*, 2009, **3**, 3339-3342.
8 G. Pérez-Mitta, J. S. Tuninetti, W. Knoll, C. Trautmann, M. E. Toimil-Molares and O. Azzaroni, *J. Amer. Chem. Soc.*, 2015, **137**, 6011-6017.
9 H. Reiss, C. S. Fuller and F. J. Morin, *Bell Systems Tech. J.*, 1956, **35**, 535-636.
10 1M. Ali, S. Nasir, P. Ramirez, J. Cervera, S. Mafe and W. Ensinger, *J. Phys. Chem. C*, 2013, **117**, 18234.
11 T. Albrecht, *ACS Nano*, 2011, **5**, 6714-6725.
12 M. Ali, I. Ahmed, S. Nasir, P. Ramirez, C. M. Niemeyer, S. Mafe and W. Ensinger, *ACS Appl. Mater. Interfaces*, 2015, **7**, 19541-19545.
13 V. Gomez, P. Ramirez, J. Cervera, S. Nasir, M. Ali, W. Ensinger and S. Mafe, *Sci. Rep.*, 2015, **5**, 9501.
14 V. Gomez, P. Ramirez, J. Cervera, S. Nasir, M. Ali, W. Ensinger and S. Mafe, *Nano Energy*, 2015, **16**, 375-382.
15 P. Apel, *Radiat. Meas.*, 2001, **34**, 559-566.
16 J. Cervera, B. Schiedt, R. Neumann, S. Mafe and P. Ramirez, *J. Chem. Phys.*, 2006, **124**, 104706.
17 A. Malvino and D. J. Bates, *Electronic Principles*, Eighth Edition, McGraw-Hill, 2015.
18 S. G. Lemay, *ACS Nano*, 2009, **3**, 775-779.
19 K. Tybrandt, R. Forchheimer and M. Berggren, *Nat. Commun.*, 2012, **3**, 871.